Isotope Effect in the Carbonyl Sulfide Reaction with O(P-3)

ARTICLE *in* THE JOURNAL OF PHYSICAL CHEMISTRY A · MARCH 2012

Impact Factor: 2.69 · DOI: 10.1021/jp2120884 · Source: PubMed

THE JOURNAL OF PHYSICAL CHEMISTRY A

Article

pubs.acs.org/JPCA

Isotope Effect in the Carbonyl Sulfide Reaction with O(^3P)

Shohei Hattori,*[,†] Johan A. Schmidt,[‡] Denise W. Mahler,[‡] Sebastian O. Danielache,[†] Matthew S. Johnson,[‡] and Naohiro Yoshida[§,†]

[†]Department of Environmental Science and Technology, Tokyo Institute of Technology, Yokohama, Japan

[‡]Copenhagen Center for Atmospheric Research, Department of Chemistry, University of Copenhagen, Universitetsparken 5, DK-2100, Copenhagen, Denmark

[§]Department of Environmental Chemistry and Engineering, Tokyo Institute of Technology, Yokohama, Japan

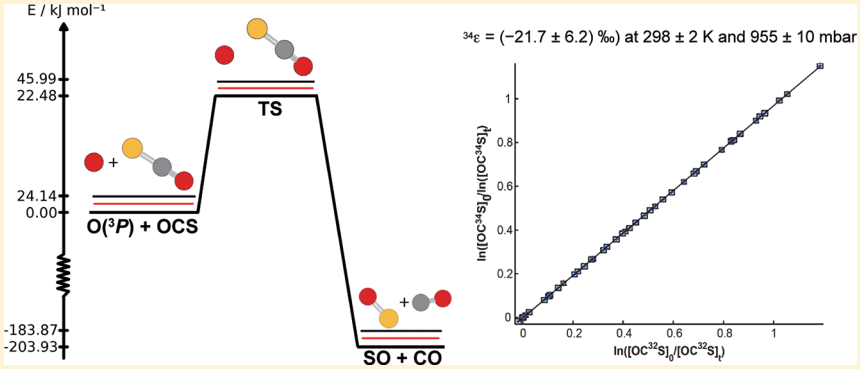

ABSTRACT: The sulfur kinetic isotope effect (KIE) in the reaction of carbonyl sulfide (OCS) with O(^3P) was studied in relative rate experiments at 298 ± 2 K and 955 ± 10 mbar. The reaction was carried out in a photochemical reactor using long path FTIR detection, and data were analyzed using a nonlinear least-squares spectral fitting procedure with line parameters from the HITRAN database. The ratio of the rate of the reaction of $OC^{34}S$ relative to $OC^{32}S$ was found to be 0.9783 ± 0.0062 ($^{34}\varepsilon$ = (−21.7 ± 6.2)‰). The KIE was also calculated using quantum chemistry and classical transition state theory; at 300 K, the isotopic fractionation was found to be $^{34}\varepsilon = -14.8$‰. The OCS sink reaction with O(^3P) cannot explain the large fractionation in ^{34}S, over +73‰, indicated by remote sensing data. In addition, $^{34}\varepsilon$ in OCS photolysis and OH oxidation are not larger than 10‰, indicating that, on the basis of isotopic analysis, OCS is an acceptable source of background stratospheric sulfate aerosol.

1. INTRODUCTION

Carbonyl sulfide (OCS) is the most abundant sulfur containing gas in the atmosphere, with an average mole fraction of 500 × 10^{-9} in the troposphere.[1] Air currents carry OCS into the stratosphere where it is decomposed by photolysis and radical reactions with OH and O(^3P).[2,3] The stratospheric sulfate aerosol (SSA) layer increases the Earth's albedo and modulates the concentration of stratospheric ozone (O_3) because of surface heterogeneous reactions.[4,5] OCS was the first species identified as a source of SSA,[6] and the cooling effect of OCS on climate, via SSA, is estimated to dominate its greenhouse effect.[7] However, Chin and Davis[8] used a 1-D model to show that atmospheric OCS is not adequate to maintain the background SSA concentration; another significant SSA source may be deep convection of SO_2 from the lower troposphere.[9−12] In contrast, Barkley et al.[13] found the stratospheric lifetime of OCS to be 64 ± 21 a from ACE satellite measurements, corresponding to a stratospheric sink of sulfur of 63 − 124 Gg a^{-1}, which matches the mass of sulfur needed to sustain the SSA, 30−170 Gg a^{-1}.[8] The background SSA source budget is not known with any certainty.

Isotopic analysis is used to trace the sources and transformations of atmospheric trace gases.[14,15] Sulfur isotopic compositions are reported as

$$\delta^{34}S = \frac{R_{sample}}{R_{standard}} - 1 \quad (1)$$

where R denotes the isotope ratios ($^{34}S/^{32}S$) of samples and standards. Isotope ratios of sulfur are reported relative to the Vienna Canyon Diablo Troilite (VCDT) standard and often denoted in per mil (‰).[16] Rather than using α to describe the isotope effect, it is common to use the isotopic fractionation constant, ε, defined as

$$\varepsilon = \alpha - 1 \quad (2)$$

The isotopic fractionation constant is reported relative to the major isotopologue (for OCS, $^{16}O^{12}C^{32}S$) and is often given in units of per mil (‰). Previous studies have considered isotopic fractionation factors of OCS photolysis[17,18] and the OCS + OH

Received: December 14, 2011
Revised: March 15, 2012
Published: March 16, 2012

reaction.[2,19] These experiments and calculations demonstrate that these two sink reactions do not have isotopic fractionations of greater than 10‰. When the estimated isotopic composition $\delta^{34}S$ (OCS) = 11‰[20] and measured $\delta^{34}S$ (SSA) = 2.6‰[21] are considered, it is seen that OCS could be an acceptable source of background SSA. However, an apparent fractionation constant for stratospheric OCS loss of 73.8 ± 8‰ in ^{34}S was reported for the lower stratosphere based on $OC^{32}S$ and $OC^{34}S$ concentration profiles obtained by the JPL MkIV limb transmittance spectrometer, seeming to show that OCS is not a dominant source of SSA.[22] Although several kinetic studies of the reaction of OCS + $O(^3P)$ have been published,[23] isotopic fractionation factors have not been reported.

In this study, we present the first measurement of the kinetic isotope effect (KIE) for the reaction of OCS with $O(^3P)$ and discuss the mechanism using ab initio calculations combined with classical transition state theory. In addition, we evaluate evidence of whether OCS is an acceptable source of background SSA; the isotopic fractionations of the three sink reactions are discussed.

2. EXPERIMENTAL METHODS

2.1. Sample Preparation. The OCS isotopologues $OC^{32}S$ and $OC^{34}S$ were synthesized from elemental sulfur using the method of Ferm.[24] This procedure involved the reaction of carbon monoxide (CO) (Japan Fine Products, 99.99% purity) with 1−5 mg of ^{32}S (99.99% isotopic enrichment) and ^{34}S (99.9% isotopic enrichment) powders (Isoflex, USA). The elemental sulfur powders were put in Pyrex glass tubes (i.d. 9 mm) and the air was evacuated. After evacuation, a stoichiometric excess of CO (2 to 3 times) was added, and the tubes were sealed. The samples were heated at 573 K for 24 h, converting S into OCS.

The product was expected to include impurities such as CO, CO_2, hydrogen sulfide (H_2S) and carbon disulfide (CS_2). The samples were purified using a gas chromatograph (GC) equipped with a thermal conductivity detector (TCD) (GC-14B; Shimadzu, Kyoto, Japan) and a packed column (Pora Pack Q, 2 mm i.d., 2.4 m) maintained at 333 K. Ultrapure He (Japan Air Gases, >99.99995% purity) was used as the carrier gas at a flow rate of 25 mL min^{-1}. The GC oven temperature program was 333 K for 8 min, rising from 333 to 473 K at a rate of 25 K min^{-1}, and then waiting 2 min at 473 K. OCS with a retention time of ca. 5.2 min was trapped at liquid nitrogen temperature (77 K) after the GC. The GC column was carefully baked between the runs to avoid contamination from other isotopologues and other components. The retention times of impurities were 3.0, 4.0, and 12.0 min for CO_2, H_2S, and CS_2, respectively. Reanalysis of the purified OCS sample confirmed that these impurities were below the detection limit (<0.1%). Purified OCS was transferred into evacuated glass tubes and stored in the dark at room temperature before experiments.

The recovery of OCS was 70−80%, and the same CO sample was used to synthesize $OC^{32}S$ and $OC^{34}S$. Since the method does not involve sulfur other than the reagent, isotopic contamination of the samples was negligible as verified with infrared spectroscopy (Bruker IFS 66 V/s) using a 10.00 cm long cell with CaF_2 windows.

2.2. Relative Rate Experiment. The kinetic study was carried out using the relative rate method in a static gas mixture in which the decays of the concentrations of the reacting species are measured simultaneously as the reaction proceeds. Consider two simultaneous bimolecular reactions of *A* and *B* with rate coefficients k_A and k_B. Assuming that there are no sources or loss processes other than these reactions, then the following relationship is valid:

$$\ln\left(\frac{[A]_0}{[A]_t}\right) = \frac{k_A}{k_B}\ln\left(\frac{[B]_0}{[B]_t}\right) \quad (3)$$

A plot of $\ln([A]_0/[A]_t)$ vs $\ln([B]_0/[B]_t)$ will thus give the kinetic isotope effect $\alpha = k_A/k_B$ as the slope. The decaying concentrations of the reactants (i.e., $OC^{32}S$ and $OC^{34}S$) are measured over time as they react with $O(^3P)$.

The experiments were carried out in a 100 L photochemical reactor installed at the University of Copenhagen.[25] This reactor was aligned to give a 64 m optical path length for Fourier transform infrared spectroscopy (FTIR) detection and is equipped with temperature control and UV−C, UV−A, and Sun lamps to photolyze gases in the reactor. All experiments were carried out in N_2 bath gas at 298 ± 1 K and 950 ± 10 mbar.

O_3 was produced from O_2 (AGA 5.0) using a 500 mg/hour O_3 generator from Ozone Technology AB. O_3 was preconcentrated on silica gel cooled with a dry ice/ethanol slurry. For $O(^3P)$ radical production, O_3 was photolyzed following eq 4.

$$O_3 + h\nu \rightarrow O_2 + O(^3P) \quad (4)$$

Broad band sun lamps (extending from 300 nm down to the IR region) were used for this purpose. OCS reacted with $O(^3P)$ according to

$$OCS + O(^3P) \rightarrow CO + SO \quad (5)$$

The initial concentrations in the photochemical reactor were 1−2 ppm of the OCS isotopologues, 800−2000 ppm O_3, and approximately 950 mbar N_2.

2.3. Analysis of Infrared Spectra and Reference Spectra. The concentration of the different species as a function of time was determined using FTIR spectroscopy. The spectra were recorded using a Bruker IFS 66v/S infrared spectrometer with a liquid-nitrogen-cooled InSb detector at a resolution of 0.13 cm^{-1}. For each spectrum, 64 scans were averaged and the interferograms were Fourier transformed using boxcar apodization. Spectra were recorded following each photolysis step of 10−20 min. The experiments were terminated when ca. 60% of OCS was consumed.

To check for possible dark reactions, the reaction mixture was left in the cell for a time corresponding to a standard experiment; no change in the concentrations of the species was observed. Photolysis tests with only OCS isotopologues in the cell did not show changes in concentration due to the lamps used to initiate the photochemistry. This is consistent with the emission spectrum of the lamp[25] and the published UV absorption cross-section of OCS.[17] Seven independent experiments were carried out, and the results were used to determine the kinetic isotope effect for the reaction.

The spectra for the different reaction mixtures were analyzed using a nonlinear least-squares spectral fitting program, MALT5 (Multi-Atmospheric Layer Transmission), developed by Griffith.[26] Parameters taken into account during the spectral fitting procedure include pressure broadening, instrument alignment, apodization, and temperature. The error in the fit is included in the determination of the slope of the relative rate plot. The spectral region was analyzed from 2000−2060 cm^{-1} for $OC^{32}S$, $OC^{34}S$, and O_3 concentrations and 2055−2160 cm^{-1} for CO concentration, respectively. In the investigated

dx.doi.org/10.1021/jp2120884 | J. Phys. Chem. A 2012, 116, 3521−3526

region (2000 to 2060 cm^{-1}), the following molecules are anticipated to absorb: OCS (fundamental C−O stretch), CO (fundamental stretch), CO_2 (fundamental asymmetric stretch and overtone and combination bands), O_3 (overtone and combination bands). Reference spectra for H_2O, O_3, CO, $^{16}O^{12}C^{32}S$, $^{16}O^{12}C^{34}S$, $^{16}O^{13}C^{32}S$, and $^{18}O^{13}C^{32}S$ were obtained from the HITRAN database.[27] For OCS isotopologues, updated line parameters from Koshelev and Tretyakov[28] were used. The data from independent experiments were analyzed according to eq 3 using a weighted least-squares procedure, which includes uncertainties in both $OC^{32}S$ and $OC^{34}S$ concentrations;[29] the uncertainties in the concentrations were taken as the standard deviations from the least-squares fitting of the experimental infrared spectra.

In addition, in order to quantify systematic errors in the fitting of the spectra, dilution experiments of OCS isotopologues were conducted, with and without O_3. A fraction of the reaction mixture was pumped out of the cell, and then, the pressure was increased back to approximately 960 mbar using N_2; ideally, this experiment will give a relative rate plot with a slope of 1.

2.4. Calculation of Rate Coefficient. The rate constants for the different isotopologues of OCS reacting with $O(^3P)$ were calculated using classical transition state theory (TST, cf. Chapter 6 of Billing and Mikkelsen[30]). The effect of tunneling was approximately taken into account using the Wigner correction[31] (cf. Chapter 8 of Billing and Mikkelsen[32]).

The relevant stationary points on the ground state potential energy surfaces (PES) were located by doing a geometry optimization using density functional theory and the B3LYP functional[33−35] together with the aug-cc-pVTZ orbital basis set.[36,37] Harmonic vibrational frequencies at the stationary points were obtained using the same level of theory for all relevant isotopologues. The reaction barrier was refined by performing single point CCSD(T)[38] calculations at the obtained reactant, transition state, and product geometries using the aug-cc-pVDZ, aug-cc-pVTZ, and aug-cc-pVQZ[36,37] basis sets followed by two extrapolations to the complete basis set limit using the scheme of Halkier et al.[39] All computational chemistry calculations were carried out using the Gaussian09 program package.[40] The reaction barrier height, energies of reactants, transition states, and products are summarized in Table 1, while harmonic frequencies and rotational constants are given in Table 4.

Table 1. Reaction Barrier and Energy of the Reactants, Transition State, and Product with and without Zero Point Energy (ZPE) Correction for the Different Isotopes[a]

	barrier height	OCS + $O(^3P)$	OC−S−O	CO + SO
no ZPE	22.4790	0	22.4790	−203.9346
(^{32}S,^{12}C)	21.8510	24.1383	45.9893	−183.8721
(^{34}S,^{12}C)	21.8562	24.0545	45.9103	−183.9390

[a]The energies were calculated using the procedure described in section 2.4 and are given in kJ mol^{-1}.

3. RESULTS AND DISCUSSION

3.1. Experimental Study. Figure 1 shows an example of the FTIR spectra obtained from a nonlinear least-squares spectral fit in the 2000−2060 cm^{-1} region using reference data from HITRAN. The residual between measured spectra and synthetic spectra calculated by MALT5 is small, and the uncertainty in the concentrations of $OC^{32}S$ and $OC^{34}S$ isotopologues were 0.6−0.8%.

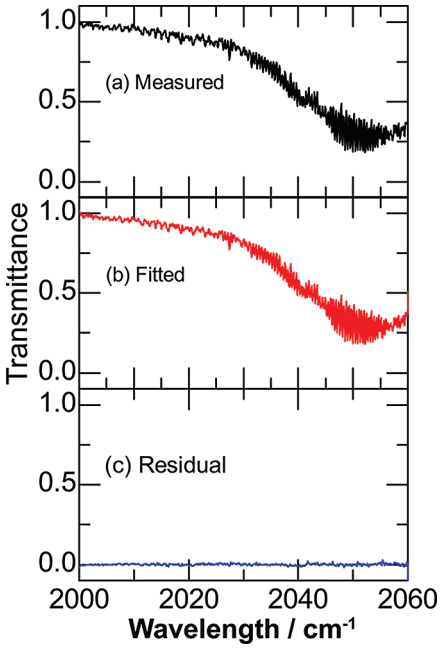

Figure 1. Example of measured and fitted spectra from an experiment.

Figure 2 shows the changes in the concentrations of O_3, CO, and OCS over the course of a typical experiment. As O_3 was photolyzed by the sun lamps to produce $O(^3P)$, the OCS reacted with the $O(^3P)$ and produced CO. The consumption of OCS and production of CO were in approximately 1:1 stoichiometry (Figure 3). Hence, the observed reaction is consistent with the reaction system of eq 5.

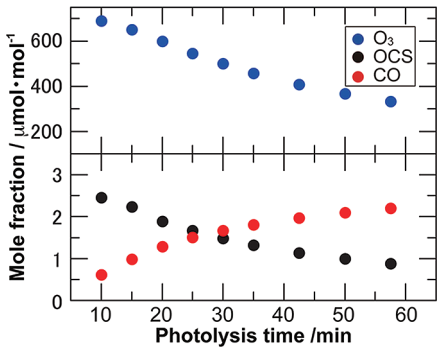

Figure 2. Changes in concentration of O_3, OCS, and CO in the reactor over the course of a typical experiment.

The plots of $\ln([OC^{32}S]_0/[OC^{32}S]_t)$ vs $\ln([OC^{34}S]_0/[OC^{34}S]_t)$ during the reaction with $O(^3P)$ radicals were analyzed in seven independent experiments according to eq 3 giving an overall result of $k(OC^{34}S + O(^3P))/k(OC^{32}S + O(^3P)) = 0.9702 \pm 0.0002$ (Figure 4). The distributions of the isotopic fractionation factors between independent experiments were independent of the amount of O_3. The average and 2 times the standard deviation (2σ) from seven independent experiments is 0.9703 ± 0.0018 ($^{34}\varepsilon = (-29.7 \pm 1.8)‰$). In the dilution experiments, the plots of $\ln([OC^{32}S]_0/[OC^{32}S]_t)$ vs $\ln([OC^{34}S]_0/[OC^{34}S]_t)$ analyzed for two independent experiments according to eq 3 gives $k(OC^{34}S)/k(OC^{32}S) = 0.9905 \pm$

dx.doi.org/10.1021/jp2120884 | J. Phys. Chem. A 2012, 116, 3521−3526

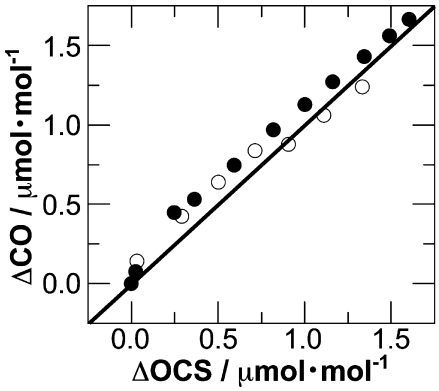

Figure 3. Correlation between OCS loss and CO production in two independent experiments.

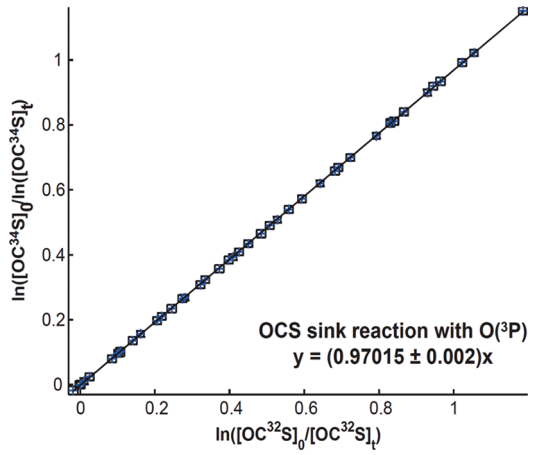

Figure 4. Relative rate plot of OCS sink reaction with $O(^3P)$ at 950 ± 10 mbar and 298 ± 2 K. Data points from seven independent experiments were fitted. The errors of the data points are smaller than size of symbols.

0.0014 in the presence of O_3, and 0.9986 ± 0.0046 without O_3. The results of the dilution experiment with and without O_3, which ideally give a relative rate plot with a slope of 1 were used to calibrate the final result. On the basis of the deviations from slope 1 in the dilution experiments, the experimental results are calibrated using estimated bias of the experiments due to overlapping absorptions by O_3. Overall, we find that the isotopic fractionation factor in ^{34}S for the OCS reaction with $O(^3P)$ is 0.9783 ± 0.0062 ($^{34}\varepsilon$ = (−21.7 ± 6.2)‰).

3.2. Computational Study. The OCS + $O(^3P)$ reaction has previously been studied using quantum chemistry.[23] The reaction can proceed via two channels, one forming SO and CO and the other forming CO_2 and S. The latter channel has a higher reaction barrier and only becomes important at temperatures exceeding 1000 K. We therefore only considered the SO + CO channel.

Table 2 compares our theoretical rate constant and Arrhenius parameters to previous experimental values. Given the simple nature of the theoretical model, the agreement with experimental values is quite satisfactory for the purpose of investigating the sulfur KIE. The theoretical rate at room temperature is about a factor 3 smaller than the experimental rates; it is not unusual for kinetic isotope effects to be predicted much more accurately than absolute rates as the rates are highly sensitive to variations in calculated energies. An error of just 3 kJ mol^{-1} in the activation barrier will cause the rate constant to be off by a factor of 3.

Table 3 shows the theoretical fractionation constants at two temperatures. The room temperature fractionation constants compare very well with our experimental results. Within classical TST, the relative rate can be factorized into three terms,

$$\alpha = f_{tun} f_Q f_{ZPE} \quad (6)$$

where f_{tun} is the ratio of the Wigner tunneling correction terms, f_Q is the ratio of the partition function terms, and f_{ZPE} is the exponential to the difference in activation barrier (due to differences in ZPE).

3.3. Atmospheric Implications. Our result shows that the OCS sink reaction with $O(^3P)$ gives a negative $^{34}\varepsilon$ of approximately −22‰. However, reactions in the stratosphere will occur at lower temperature and pressure than the conditions of this experiment. The OCS sink reaction with

Table 3. Fractionation Constant, Tunneling, Partition Function, and ZPE Factors (See Text)

	200 K	300 K
$^{34}\varepsilon$	−18.0‰	−14.8‰
$^{34}f_{tun}$	0.9972	0.9986
$^{34}f_Q$	0.9880	0.9886
$^{34}f_{ZPE}$	0.9968	0.9979

Table 4. Vibrational Frequencies and Rotational Constants for Reactants, Transition States, and Products[a]

species	frequencies (cm^{-1})	rotational constants (cm^{-1})
$O^{12}C^{32}S$	526.822[b] (520.197), 873.708 (866.367), 2108.270 (2072.140)	0.203 (0.203)
$O^{12}C^{34}S$	526.027[b] (519.424), 861.886 (854.738), 2107.672 (2071.529)	0.197 (0.198)
$O^{12}C-{}^{32}S-O$	*i*265.686, 115.029, 429.795, 495.272, 815.766, 2074.850	0.101, 0.123, 0.582
$O^{12}C-{}^{34}S-O$	*i*262.812, 114.349, 429.685, 494.425, 804.719, 2074.405	0.100, 0.122, 0.566
^{32}SO	1146.701 [1149.2]	0.703 [0.721]
^{34}SO	1135.413	0.689
^{12}CO	2207.518 [2169.8]	1.940 [1.931]

[a]The experimental data given in parentheses and brackets is from Masukidi et al.[43] and Herzberg,[44] respectively. [b]Doubly degenerate.

Table 2. Rate Constant and Arrhenius Parameters, $k = A\exp(-E_b/RT)$

	k (300 K)	A (cm^3 s^{-1})	E_b (kJ mol^{-1})	note
this study	3.69×10^{-15}	2.35×10^{-11}	21.8510	at 300 K
Aktinson et al.[41]	1.22×10^{-14}	1.6×10^{-11}	17.9	230−500 K
Singleton and Cvetanović[42]	1.25×10^{-14}	7.80×10^{-11}	21.8	230−1900 K

dx.doi.org/10.1021/jp2120884 | J. Phys. Chem. A 2012, 116, 3521−3526

$O(^3P)$ is a bimolecular metathesis reaction and is not expected to be dependent on pressure. Furthermore, the transition state theory calculation shows that the temperature dependence of the KIE is less than the experimental error, −3‰ as temperature goes from 300 to 200 K. We therefore use the experimental isotopic fractionation constant for discussing the atmospheric implications.

From previous studies based on absorption cross-section measurements of OCS isotopologues[17] and a laboratory experiment of OCS photolysis,[18] it is known that OCS photolysis does not produce isotopic fractionation greater than 10‰. In addition, isotopic fractionation of ^{34}S in the OCS sink reaction with OH radicals was estimated by a theoretical calculation to be −2.56‰.[2,19] In the present work, we report negative $^{34}\varepsilon$ in the OCS reaction with $O(^3P)$. Hence, atmospheric OCS sink reactions are not able to produce large positive isotopic fractionations in ^{34}S. The reported isotopic fractionation of ^{34}S of (+73.8 ± 8.6)‰ in OCS decomposition for the lower stratosphere derived using stratospheric $OC^{34}S$ and $OC^{32}S$ concentration profiles from the infrared limb transmittance spectra acquired by the JPL MkIV instrument may perhaps be due to retrieval error.[22]

The $\delta^{34}S$ value of 11‰ in tropospheric OCS was estimated by considering the mass balance of oceanic sulfur and terrestrial sulfur sources.[20] The OCS oxidation product, background SSA, is reported to be $\delta^{34}S$ = 2.6‰,[21] indicating that background SSA is less enriched in ^{34}S than tropospheric OCS. Our results and literature data show that the OCS sink reactions give only a small and/or negative isotopic fractionation. Consequently, sulfate from OCS sink reactions will not be enriched (by more than 5‰) but rather depleted in ^{34}S compared to the initial material, showing that OCS is an acceptable source of background SSA.

4. CONCLUSIONS

The main result of this study is that the OCS reaction with $O(^3P)$ produces a negative KIE in ^{34}S. Together with other isotopic studies of OCS photolysis[17,18] and OCS reaction with OH,[2] we are now able to revise the conclusion of an earlier study that used isotopes to show that the composition of SSA was not consistent with an OCS photooxidation source.[22] Sulfate from OCS sink reactions will not be enriched (by more than 5‰) but rather depleted in ^{34}S compared to the initial material based on isotopic fractionations in three OCS sink reactions, showing that OCS is indeed an acceptable source of background SSA. In the future, modeling of isotopic fractionations of the OCS sink reaction is needed for better understanding of the possibility of OCS as a source of background SSA.

AUTHOR INFORMATION

Corresponding Author

*E-mail: hattori.s.ab@m.titech.ac.jp.

Notes

The authors declare no competing financial interest.

ACKNOWLEDGMENTS

We wish to thank R. Forecast and J. Heimdal for assistance with experiments. This work is supported by Global Environmental Research Fund (A-0904) of the Ministry of the Environment, Japan, and Grant in Aid for Scientific Research (S) (23224013) of Ministry of Education, Culture, Sports, and Technology (MEXT), Japan. The research also has received funding from the European Community's Seventh Framework Programme (FP7/2007-2013) under grant agreement number 237890. S.H. is supported by Grant in Aid for JSPS Research Fellows (DC1 (No.22-7563)) and Global COE program "Earth to Earths" of MEXT, Japan.

REFERENCES

(1) Watts, S. F. *Atmos. Environ.* **2000**, *34*, 761−779.
(2) Danielache, S. O.; Johnson, M. S.; Nanbu, S.; Grage, M. M. L.; McLinden, C.; Yoshida, N. *Chem. Phys. Lett.* **2008**, *450*, 214−220.
(3) McKee, M. L.; Wine, P. H. *J. Am. Chem. Soc.* **2001**, *123*, 2344−2353.
(4) Junge, C. E. *Tellus* **1966**, *18*, 685−685.
(5) Myhre, G.; Berglen, T. F.; Myhre, C. E. L.; Isaksen, I. S. A. *Tellus, Ser. B* **2004**, *56*, 294−299.
(6) Crutzen, P. J. *Geophys. Res. Lett.* **1976**, *3*, 73−76.
(7) Brühl, C.; Lelieveld, J.; Crutzen, P. J.; Tost, H. *Atmos. Chem. Phys.* **2012**, *12*, 1239−1253.
(8) Chin, M.; Davis, D. D. *J. Geophys. Res.* **1995**, *100*, 8993−9005.
(9) Weisenstein, D. K.; Yue, G. K.; Ko, M. K. W.; Sze, N.-D.; Rodriguez, J. M.; Scott, C. J. *J. Geophys. Res.* **1997**, *102*, 13019−13035.
(10) Kjellström, E. *J. Atmos. Chem.* **1998**, *29*, 151−177.
(11) Pitari, G.; Mancini, E.; Rizi, V.; Shindell, D. T. *J. Atmos. Sci.* **2002**, *59*, 414−440.
(12) Stevenson, D. S.; Johnson, C. E.; Collins, W. J.; Derwent, R. G. *Spec. Publ., Geol. Soc. Lond.* **2003**, *213*, 295−305.
(13) Barkley, M. P.; Palmer, P. I.; Boone, C. D.; Bernath, P. F.; Suntharalingam, P. *Geophys. Res. Lett.* **2008**, *35* (L14810), 7.
(14) Johnson, M. S.; Feilberg, K. L.; Hessberg, P. V.; Nielsen, O. J. *Chem. Soc. Rev.* **2002**, *31*, 313−323.
(15) Brenninkmeijer, C. A. M.; Janssen, C.; Kaiser, J.; Röckmann, T.; Rhee, T. S.; Assonov, S. S. *Chem. Rev.* **2003**, *103*, 5125−5162.
(16) Hoefs, J. *Stable Isotope Geochemistry*, 6th ed; Springer: Berlin, Germany, 2009.
(17) Hattori, S.; Danielache, S. O.; Johnson, M. S.; Schmidt, J. A.; Kjaergaard, H. G.; Toyoda, S.; Ueno, Y.; Yoshida, N. *Atmos. Chem. Phys.* **2011**, *11*, 10293−10303.
(18) Lin, Y.; Sim, M. S.; Ono, S. *Atmos. Chem. Phys.* **2011**, *11*, 10283−10292.
(19) Schmidt, J. A.; Johnson, M. S.; Jung, Y.; Danielache, S. O.; Hattori, S.; Yoshida, N. *Chem. Phys. Lett.* **2012**, *531*, 64−69.
(20) Krouse, H. R.; Grinenko, V. A. *Stable Isotopes: NAACO*; Scope John Wiley and Sons: New York, 1991. http://www.icsu-scope.org/downloadpubs/scope43/index.html (accessed Mar 15, 2012).
(21) Castleman, A. J.; Munkelwitz, H.; Manowitz, B. *Tellus* **1974**, *26*, 222−234.
(22) Leung, F.-Y. T.; Colussi, A. J.; Hoffmann, M. R.; Toon, G. C. *Geophys. Res. Lett.* **2002**, *29* (1474), 4.
(23) Chiang, H.-C.; Wang, N.-S.; Tsuchiya, S.; Chen, H.-T.; Lee, Y.-P.; Lin, M. C. *J. Phys. Chem. A* **2009**, *113*, 13260−13272.
(24) Ferm, R. J. *Chem. Rev.* **1957**, *57*, 621−640.
(25) Nilsson, E. J. K.; Eskebjerg, C.; Johnson, M. S. *Atmos. Environ.* **2009**, *43*, 3029−3033.
(26) Griffith, D. W. T. *Appl. Spectrosc.* **1996**, *50*, 59−70.
(27) Rothman, L. S.; Jacquemart, D.; Barbe, A.; Chris Benner, D.; Birk, M.; Brown, L. R.; Carleer, M. R.; Chackerian, J. C.; Chance, K.; Coudert, L. H.; Dana, V.; Devi, V. M.; Flaud, J. M.; Gamache, R. R.; Goldman, A.; Hartman, J. M.; Jucks, J. W.; Maki, A. G.; Mandin, J. Y.; Massie, S. T.; Orphal, J.; Perrin, A.; Rinsland, C. P.; Smith, M. A. H.; Tennyson, J.; Tolchenov, R. N.; Toth, R. A.; Vander Auwera, J.; Varanasi, P.; Wagner, G. *J. Quant. Spectrosc. Radiat. Transfer* **2005**, *96*, 139−204.
(28) Koshelev, M. A.; Tretyakov, M. Y. *J. Quant. Spectrosc. Radiat. Transfer* **2009**, *110*, 118−128.
(29) York, D. *Can. J. Phys.* **1966**, *44*, 1079−1086.

(30) Billing, G. D.; Mikkelsen, K. V. *Introduction to Molecular Dynamics and Chemical Kinetics*; Wiley-Interscience Publication: Copenhagen, Denmark, 1996.
(31) Wigner, E. P. *Z. Phys. Chem.* **1932**, *B19*, 203−216.
(32) Billing, G. D.; Mikkelsen, K. V. *Advanced Molecular Dynamics and Chemical Kinetics*; Wiley-Interscience Publication: Copenhagen, Denmark, 1997.
(33) Becke, A. D. *J. Chem. Phys.* **1993**, *98*, 5648−5652.
(34) Lee, C.; Yang, W.; Parr, R. G. *Phys. Rev. B* **1988**, *37*, 785−789.
(35) Stephens, P. J.; Devlin, F. J.; Chabalowski, C. F.; Frisch, M. J. *J. Phys. Chem.* **1994**, *98*, 11623−11627.
(36) Dunning, T. H. J. *J. Chem. Phys.* **1989**, *90*, 1007−1023.
(37) Woon, D. E.; Dunning, T. H. J. *J. Chem. Phys.* **1993**, *98*, 1358−1371.
(38) Watts, J. D.; Gauss, J.; Bartlett, R. J. *J. Chem. Phys.* **1993**, *98*, 8718−8733.
(39) Halkier, A.; Helgaker, T.; Jørgensen, P.; Klopper, W.; Koch, H.; Olsen, J.; Wilson, A. K. *Chem. Phys. Lett.* **1998**, *286*, 243−252.
(40) Frisch, M. J.; Trucks, G. W.; Schlegel, H. B.; Scuseria, G. E.; Robb, M. A.; Cheeseman, J. R.; Scalmani, G.; Barone, V.; Mennucci, B.; Petersson, G. A.; Nakatsuji, H.; Caricato, M.; Li, X.; Hratchian, H. P.; Izmaylov, A. F.; Bloino, J.; Zheng, G.; Sonnenberg, J. L.; Hada, M.; Ehara, M.; Toyota, K.; Fukuda, R.; Hasegawa, J.; Ishida, M.; Nakajima, T.; Honda, Y.; Kitao, O.; Nakai, H.; Vreven, T.; Montgomery, J. A., Jr.; Peralta, J. E.; Ogliaro, F.; Bearpark, M.; Heyd, J. J.; Brothers, E.; Kudin, K. N.; Staroverov, V. N.; Kobayashi, R.; Normand, J.; Raghavachari, K.; Rendell, A.; Burant, J. C.; Iyengar, S. S.; Tomasi, J.; Cossi, M.; Rega, N.; Millam, J. M.; Klene, M.; Knox, J. E.; Cross, J. B.; Bakken, V.; Adamo, C.; Jaramillo, J.; Gomperts, R.; Stratmann, R. E.; Yazyev, O.; Austin, A. J.; Cammi, R.; Pomelli, C.; Ochterski, J. W.; Martin, R. L.; Morokuma, K.; Zakrzewski, V. G.; Voth, G. A.; Salvador, P.; Dannenberg, J. J.; Dapprich, S.; Daniels, A. D.; Farkas, O.; Foresman, J. B.; Ortiz, J. V.; Cioslowski, J.; Fox, D. J. *Gaussian 09*, revision A.1; Gaussian, Inc.: Wallingford, CT, 2009.
(41) Atkinson, R.; Baulch, D. L.; Cox, R. A.; Crowley, J. N.; Hampson, R. F. J.; Hynes, R. G.; Jenkin, M. E.; Kerr, J. A.; Rossi, M. J.; Troe, J. *Summary of Evaluated Kinetic and Photochemical Data for Atmospheric Chemistry*; Centre for Atmospheric Science, University of Cambridge: Cambridge, U.K., 2006. http://rpw.chem.ox.ac.uk/IUPACsumm_web_latest.pdf (accessed Mar 15, 2012).
(42) Singleton, D. L.; Cvetanović, R. J. *J. Phys. Chem. Ref. Data* **1988**, *17*, 1377 and reference therein..
(43) Masukidi, L. S.; Lahaye, J. G.; Fayt, A. *J. Mol. Spectrosc.* **1992**, *154*, 137−162.
(44) Huber, K. P.; Herzberg, G. *Molecular Spectra and Molecular Structure, IV. Constants of Diatomic Molecules*; Van Nostrand Reinhold Company: New York, 1978.